

This is the peer reviewed version of the following article:

First-Principles Insights into the Structural and Electronic Properties of Polytetrafluoroethylene in Its High-Pressure Phase (Form III) / Fatti, Giulio; Righi, M. C.; Dini, Daniele; Ciniero, Alessandra. - In: JOURNAL OF PHYSICAL CHEMISTRY. C. - ISSN 1932-7447. - 123:10(2019), pp. 6250-6255. [10.1021/acs.jpcc.8b11631]

*Terms of use:*

The terms and conditions for the reuse of this version of the manuscript are specified in the publishing policy. For all terms of use and more information see the publisher's website.

17/12/2025 20:04

## First-Principles Insights into the Structural and Electronic Properties of PTFE in its High-Pressure Phase (Form III)

Giulio Fatti, Maria Clelia Righi, Daniele Dini, and Alessandra Ciniero

*J. Phys. Chem. C*, **Just Accepted Manuscript** • DOI: 10.1021/acs.jpcc.8b11631 • Publication Date (Web): 21 Feb 2019

Downloaded from <http://pubs.acs.org> on February 25, 2019

### Just Accepted

"Just Accepted" manuscripts have been peer-reviewed and accepted for publication. They are posted online prior to technical editing, formatting for publication and author proofing. The American Chemical Society provides "Just Accepted" as a service to the research community to expedite the dissemination of scientific material as soon as possible after acceptance. "Just Accepted" manuscripts appear in full in PDF format accompanied by an HTML abstract. "Just Accepted" manuscripts have been fully peer reviewed, but should not be considered the official version of record. They are citable by the Digital Object Identifier (DOI®). "Just Accepted" is an optional service offered to authors. Therefore, the "Just Accepted" Web site may not include all articles that will be published in the journal. After a manuscript is technically edited and formatted, it will be removed from the "Just Accepted" Web site and published as an ASAP article. Note that technical editing may introduce minor changes to the manuscript text and/or graphics which could affect content, and all legal disclaimers and ethical guidelines that apply to the journal pertain. ACS cannot be held responsible for errors or consequences arising from the use of information contained in these "Just Accepted" manuscripts.



# First-Principles Insights into the Structural and Electronic Properties of PTFE in its High-Pressure Phase (Form III)

Giulio Fatti<sup>†</sup>, M. Clelia Righi<sup>†, ‡</sup>, Daniele Dini<sup>§</sup>, Alessandra Ciniero<sup>\*, †, §</sup>

<sup>†</sup>Department of Physics, Informatics and Mathematics, University of Modena and Reggio Emilia, Via Campi, 213/A 41125 Modena, Italy

<sup>‡</sup>CNR-Institute of Nanoscience, S3 Center, Via Campi 213/A, 41125 Modena, Italy

<sup>§</sup>Tribology Group, Department of Mechanical Engineering, Imperial College London, London SW7 2AZ, UK

## ABSTRACT

Polytetrafluoroethylene (PTFE), commercially known as Teflon, is one the most effective insulating polymers for a wide range of applications, due to its peculiar electronic, mechanical and thermal properties. Several studies have attempted to elucidate the structural and electronic properties of PTFE, however, some important aspects of its structural and electronic characteristics are still under debate. To shed light on these fundamental features we have employed a first-principles approach to optimize the two coexisting PTFE structures (monoclinic and orthorhombic) at high pressure by using the characteristic zigzag planar chain configuration. Our electronic analysis of the optimized structures shows charge transfer from carbons to fluorines supporting the PTFE electronegativity character. In addition, band structure calculations show that the band gap is estimated around 5eV, which correlates with previous studies. Moreover, the analysis of the valence and conduction states reveals an intra-chain and an inter-chain character of the charge distribution suggesting additional insights into the PTFE electronic properties.

## 1. INTRODUCTION

PTFE is the most used polymer for a number of technologies which require specific mechanical, electrical, chemical and thermal properties. It is widely used for its low friction and wear, chemical inertness, resistance to adhesion, hydrophobicity and biocompatibility.

Nowadays, PTFE is the most popular insulating polymer for triboelectric applications, such as harvesting devices<sup>1-2</sup>. These are based on contact-induced electrification effects by which certain materials become electrically charged after they come into frictional contact with a different material<sup>3-11</sup>. Despite thousands of years of research on triboelectrification, the phenomenon is still being studied and debates still arise over aspects of the mechanisms behind it<sup>12</sup>. Recent studies, for example, disputed the

unidirectional transfer of charge by showing a mosaic distribution of charge<sup>10, 13-14</sup>, that is likely due to mechanochemical reactions<sup>15</sup>.

In addition to triboelectric technologies other industrial applications employed PTFE as material for components such as sliding<sup>16</sup> and dry bearings<sup>17</sup> and Teflon beads<sup>18</sup> and for all of them PTFE experiences high pressure conditions.

It is known that PTFE properties are based on the interaction of fluorinate carbon species, where the fluorine high electronegativity generates quite polar C-F bonds. Moreover, the presence of fluorine significantly influences intermolecular interactions which are consistent with high thermal and chemical stabilities<sup>19</sup>.

To better understand these properties, obtaining a clearer understanding of the electronic structure of PTFE is mandatory. Despite the fact that several combined experimental and theoretical studies<sup>20-31</sup> and various calculations<sup>32-39</sup> have been reported, the most important characteristics regarding the structural and electronic nature of this polymer, in particular, under high pressure conditions for discussing the electric and electronic properties could not be clearly determined. For instance, previous first-principles studies on the structural characterization of the PTFE focused only on its hexagonal crystal structure<sup>34</sup>. Therefore, there is a lack of information regarding the monoclinic and orthorhombic crystal structures which exist at high pressure conditions. The electronic properties were, instead, previously defined only for single chain<sup>24, 31, 39</sup> lacking information on the electronic interactions between the chains.

PTFE, consisting wholly of carbon (C) and fluorine (F), shows a peculiar polymorphic behavior involving three unique crystalline phases. The two crystalline phases at low pressure and temperature are usually denoted as form II consisting of helical chains containing 13 CF<sub>2</sub> in 6 turns and stable at temperatures lower than 19 °C and form IV consisting of helical chains contain 15 CF<sub>2</sub> in 7 turns and stable at temperature between 19 and 30 °C. These phases have been studied extensively and are relatively well understood<sup>40-42</sup>. The third phase, called form III, observed above ~0.65 GPa, consists of zigzag planar chains and it is stable at temperatures higher than 30°C up to the melting point of 330°C<sup>43</sup>. Spectroscopic data indicated that at pressures above 0.65 GPa the molecules untwist from the low pressure helical conformation to the planar zigzag conformation of phase III<sup>44</sup>. X-ray diffraction measurements on form III have indicated a monoclinic structure<sup>45</sup>, whereas another X-ray study<sup>25</sup> has indicated a structure similar to that of orthorhombic polyethylene (PE). An additional study<sup>46</sup>, which adopted a range of pressures between 0.95 and 5.2 GPa at 300 K found that from a pressure of 2 GPa onwards a monoclinic crystal structure coexists with an orthorhombic crystal structure.

Here, we present, for the first time, insights into structural and electronic properties of PTFE in its high-pressure phase by a first-principles approach. In our study phase III plane zigzag chains containing 8 CF<sub>2</sub> units are packed in a monoclinic and orthorhombic crystal structure and three different exchange-correlation functionals (PZ, PBE and PBE-D) are compared. Crystal structure parameters, atomic positions, bond lengths, bond angles, cohesive energy density and binding energy are calculated

and compared with literature values. The optimized structures are then used to determine the electronic states and the charge density distribution within the crystal.

## 2. COMPUTATIONAL DETAILS

Density Functional Theory (DFT) as implemented in the Quantum ESPRESSO package was used to perform first-principles calculations to describe the structural and electronic properties of PTFE bulk. We adopted and compared results from i) local density approximation (LDA), with the Perdew-Zunger (PZ) exchange-correlation functional<sup>47</sup>, ii) general gradient approximation (GGA), with the Perdew-Burke-Ernzerhof (PBE) exchange-correlation functional<sup>48</sup>, iii) and the same PBE functional corrected by a dispersion term (PBE-D) to model the long range van der Waals (vdW) interactions. The dispersion term was introduced using semi-empirical Grimme method<sup>49</sup> which is characterized by two parameters, scaling parameter and vdW cut-off radius. This dispersion term was tuned to obtain accurate structural parameters and to reproduce experimental binding energy values. The atomic species were described by ultrasoft pseudopotentials and the electronic wave functions were expanded in plane-waves.

The structural and electronic properties were analyzed with the focus on high pressure (above 0.65 GPa), at which it is known that PTFE assumes a zigzag chain conformation<sup>46</sup> in coexisting orthorhombic and monoclinic crystal structures<sup>25, 38</sup>. Therefore, we considered and compared the PTFE properties of these two different configurations. In addition, the outcomes of orthorhombic structure analysis allowed us to make a direct comparison with the results of the same structure of PE<sup>30, 50</sup>, another polymer which is extensively used due to similar electronic properties.

The PTFE stem was first optimized by performing an energy convergence test. The isolated stem was studied by introducing a vacuum of 30 Å on each side of the stem, to prevent any interaction between the periodic replicas. We found an optimal length of 8 CF<sub>2</sub> monomers.

The optimized stem was then employed for the structural properties analysis. The calculations for monoclinic structure were performed on a 2 × 1 cell to obtain the same degrees of freedom as in the unitary orthorhombic cell and provide an accurate comparison between the two geometries (Figure 1a, b). Monkhorst-Pack grids<sup>51</sup> with 2 × 2 × 4 and 2 × 3 × 4 k-points sampling were used to sample the Brillouin zone of the monoclinic and orthorhombic cell, respectively.

The electronic properties were calculated using the optimized crystal structures and the partial charges of the atoms were computed by means of the Bader analysis<sup>52-55</sup>.

## 3. RESULTS AND DISCUSSION

### 3.1. Structures optimization

An initial optimization of the lattice structures was conducted to provide a good description of the two high pressure configurations of the PTFE. The structure of the two cells and the stem used for the calculations is shown in Figure 2. The long horizontal edge and the short vertical edge of both monoclinic and orthorhombic cell are indicated by the lattice parameters  $a$  and  $b$ , respectively (Figure 1a, b), and the stems length is defined by the parameter  $c$  (Figure 1c). The angle of the monoclinic cell is indicated by the parameter  $\gamma$  (Figure 1a). In the orthorhombic configuration, PTFE stems are tilted by a setting angle with respect to the  $b$  axis (Figure 1b).

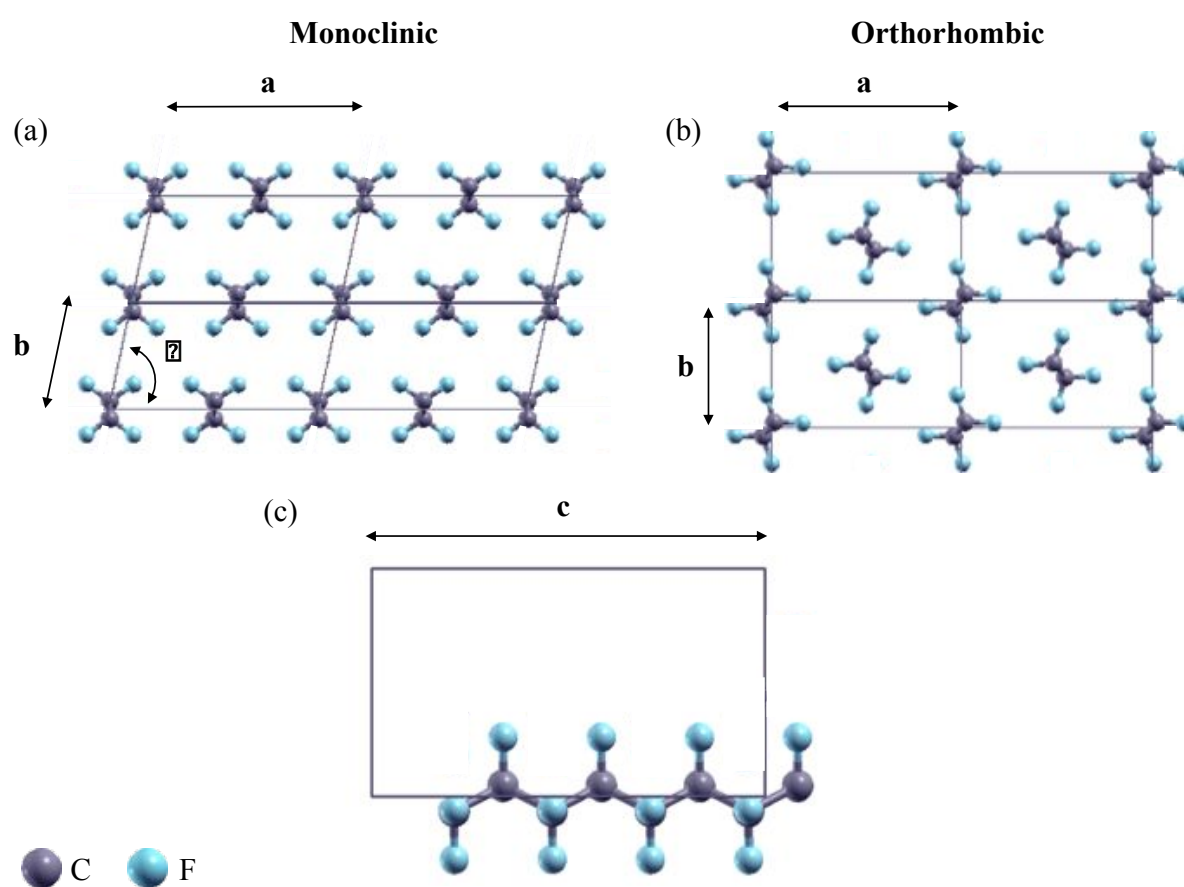


**Figure 1.** PTFE configurations at high pressure (a) monoclinic structure and (b) orthorhombic structure and (c) length of the PTFE stem

The following steps were adopted to identify the convergence cut-off for the plane-wave expansion and optimize the two cells structure. Firstly, the cells parameters were set as found in literature<sup>56</sup>. Then the structures were relaxed, varying the lattice parameter  $c$ , while performing a convergence test on the cut-off. For each cut-off, the energy values at  $c$  were fitted by the Murnaghan equation of states<sup>57</sup> to find the minimum energy configuration. Although the Murnaghan equation of states is limited

in the way it describes non-elastic behavior, in the case of PTFE, far away from the equilibrium, we strongly believe that it is suitable to describe a configuration close to the equilibrium. We found an optimum cut-off value of 40 Ry (320) for the wave functions (electron density).

Using the obtained cut-off and the equilibrium value of  $c$ , we then optimized the lattice parameters  $a$  and  $b$  for both cells, and  $\gamma$  for the monoclinic cell, using the same fitting procedure. Table 1 shows the parameters values of the optimized structures, together with the intramolecular bond lengths and angles, Cohesive Energy Density (CED) and binding energy ( $E_b$ ) per monomer. For PBE-D the scaling parameter of the vdW correction was tuned to a value of 0.42 to reproduce a CED consistent with the experimental data.

**Table 1.** Summary of the crystal structure parameters ( $a$ ,  $b$ ,  $c$  and  $\gamma$ ), atomic positions, setting angle, bond lengths, bond angles, cohesive energy density (CED) and binding energy ( $E_b$ ) of the optimized monoclinic and orthorhombic structure and experimental literature values

	Monoclinic				Orthorhombic			
	PZ	PBE	PBE-D	Exp.	PZ	PBE	PBE-D	Exp.
$a$ [Å]	9.64	10.10	9.79	9.50 <sup>36</sup> /9.04 <sup>35</sup> 8.52 <sup>38</sup> /9.44 <sup>38</sup>	8.54	9.14	8.70	8.73 <sup>21</sup>
$b$ [Å]	5.17	5.60	5.15	5.05 <sup>36</sup> /5.29 <sup>38</sup> 5.08 <sup>38</sup> /5.03 <sup>38</sup>	5.79	6.14	5.97	5.69 <sup>21</sup>
$c$ [Å]	10.38	10.65	10.61	10.48 <sup>36</sup>	10.38	10.64	10.61	---
$\gamma$ [deg]	104.7	102.4	101.8	105.5 <sup>38</sup>	---	---	---	---
setting angle [deg]	---	---	---	---	42/40	37/38	37/38	35 <sup>38</sup>
C-C [Å]	1.56	1.59	1.58	1.541 <sup>36</sup>	1.55	1.58	1.58	1.541 <sup>21</sup>
C-F [Å]	1.34	1.36	1.36	1.344 <sup>36</sup>	1.34	1.36	1.36	1.344 <sup>21</sup>
C-C-C [deg]	112.86	114.0	113.7	116.6 <sup>36</sup>	112.93	113.9	113.8	---
F-C-F [deg]	109.5	109.0	109.3	109.5 <sup>36</sup>	109.5	109.0	109.08	108.5 <sup>21</sup>
CED [N/cm <sup>2</sup> ]	309.9	15.6	194.2	185 <sup>22</sup> /196 <sup>23</sup>	229.2	31.0	194.3	185 <sup>22</sup> /196 <sup>23</sup>
$E_b$ [eV]	0.097	0.014	0.081	---	0.120	0.007	0.083	---

In both monoclinic and orthorhombic cells, *a* and *b* parameters are adequately described by PZ and PBE-D functionals, whereas they are overestimated by PBE. This was expected due to the fact that PBE overlooks long-range interactions, and this is also confirmed by the significantly low CED.

The stem length, *c*, estimated by PZ is, as expected, lower compared to that obtained using PBE and PBE-D, because PZ generally overestimates the interaction energies. This is also reflected in the smaller backbone C-C-C angle and in the higher CED.

Likewise, PBE and PBE-D underestimate the backbone angle. We attribute this discrepancy to the intermolecular interactions, absent or at least different in nature in the previous studies that adopted single chain or hexagonal cell<sup>36-37</sup>.

The C-C and C-F bond lengths as well as the F-C-F angle are well described by all the functionals. In the orthorhombic cell the setting angle is slightly overestimated by PBE-D and PZ, while significantly overestimated by PBE.

Finally, the last row of Table I shows that the binding energy between the two stems is similar for both monoclinic and orthorhombic cell. Therefore, we can confirm the coexistence of the two structures.

Overall, we can conclude that PZ overestimates the short-range interactions and PBE completely overlooks the intermolecular interactions. Instead, PBE-D characterizes correctly both short and long-range interactions, providing an accurate description of all the parameters. It can, therefore, be considered the functional which better describes the structural properties of PTFE in the high-pressure configurations.

### 3.2. Electronic properties

To provide insights into the electronic properties of both the monoclinic and orthorhombic PTFE structures we began by calculating the charge density distribution and the partial charges of the atoms.

The outcomes show the transfer of electronic charge from carbons to fluorines inside the monomers which is due to the difference of electronegativity between the two atoms (3.98 - fluorine, 2.55 - carbon).

The partial charges do not differ either between PZ, PBE and PBE-D functionals, or between the orthorhombic and monoclinic structures; the fluorines in the CF<sub>2</sub> monomer accumulate ~0.86 electron charge, while carbon loses ~1.72 electron charge.

We, then, calculated and compared the band structure of the two considered cells for each adopted functionals. The monoclinic and orthorhombic band structures for each functionals are shown in Figure 2a,c, respectively.



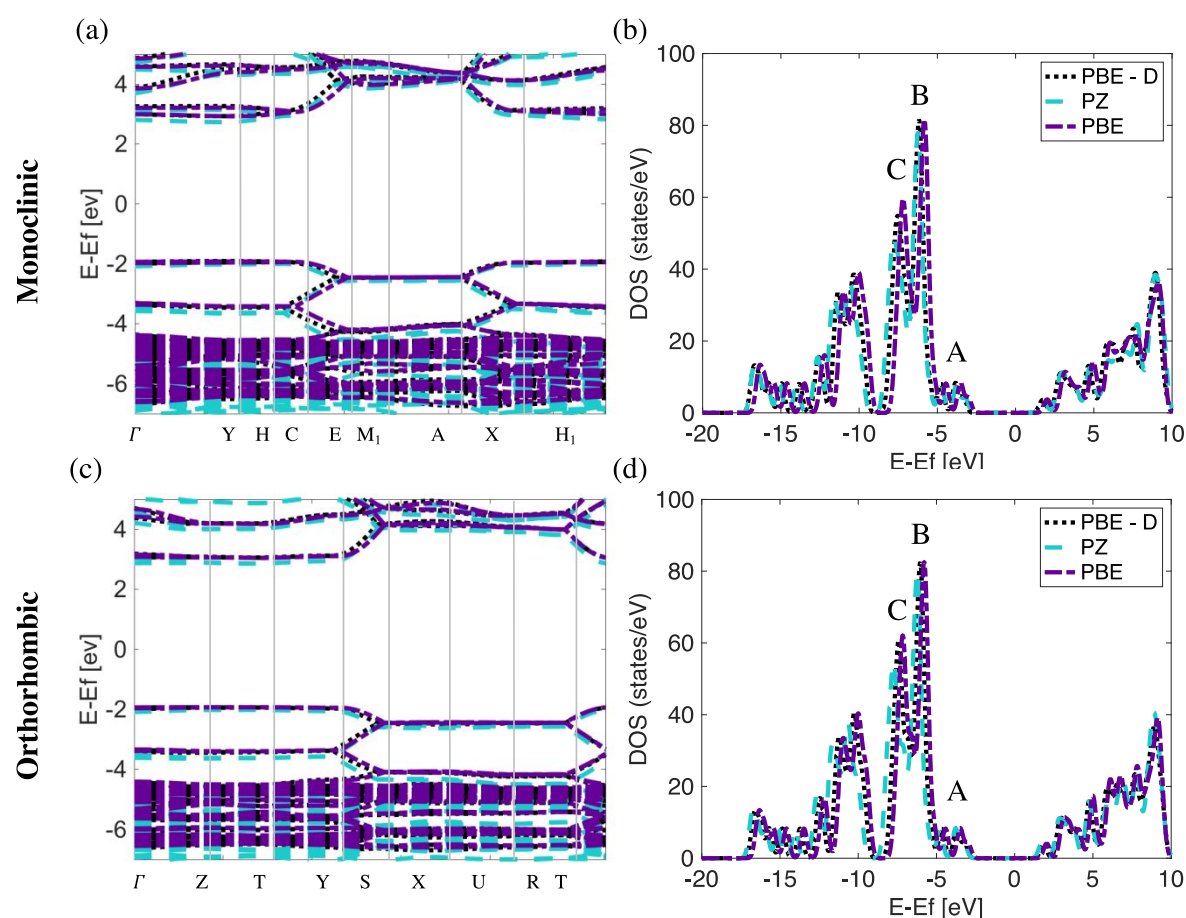


**Figure 2.** Band structure and DOS's of (a) and (b) monoclinic structure for PZ, PBE and PBE-D functional and (c) and (d) orthorhombic structure for PZ, PBE and PBE-D functional

For both monoclinic and orthorhombic structures and for each employed functional the band gap is estimated around 5 eV, in good agreement with experimental measurements ( $\sim 6$  eV)<sup>28-29</sup>. However, the calculated value is lower when compared to previous theoretical studies ( $\sim 8$  eV)<sup>34</sup> and experimental UPS and optical measurements ( $\sim 10$  eV)<sup>24</sup>.

This difference between theoretical (DFT) and experimental values was expected because of the well-known "band-gap problem" of LDA and GGA in the calculation of the insulating band gap<sup>58</sup>.

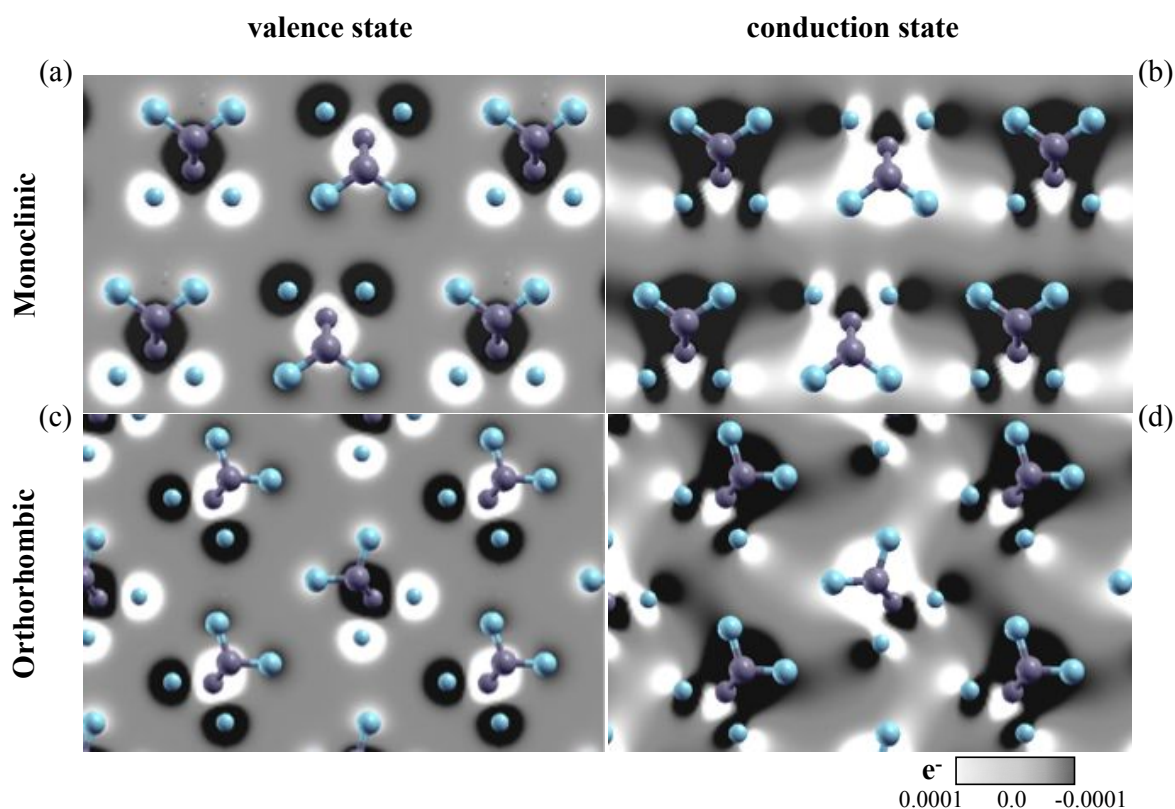
Overall, both valence and conduction bands dispersion does not differ significantly between the functionals and the cells structure adopted. In particular, for each functional and structure the band gap is direct, and little dispersion is observed at the highest occupied bands.

Figure 2b, d show the total Densities of States (DOS's) of the monoclinic and orthorhombic structure, respectively, for all the employed functionals, with the energy values in abscissa related to the Fermi energy. The peak A derives from the two highest occupied bands of Figure 2a, c which correspond to the C-C interactions. B and C, instead, derive from the high-density bands which correspond to the C-F interactions.

This agrees with previous theoretical studies on single chain in which it is suggested that the highest occupied bands are mainly derived from the interaction between the C2p and F2p levels [20].

The obtained DOS's profile aligns with previous studies reported in Ref <sup>24</sup>.

To observe the spatial configuration of both valence and conduction band additional analysis was conducted by calculating the charge density of the highest valence state and of the lowest conduction state. Figure 3 shows the results obtained with the adoption of PBE-D functional. The charge density distribution of the valence (left panel) and conduction (right) state for both monoclinic and orthorhombic structure are shown in the top and in the bottom panel, respectively. The charge distribution of the valence state (Figure 3a, c) is localized inside the PTFE stem. Inversely, the charge distribution in the conduction band is delocalized along the entire length of the chain and positioned around the C-F bonds (Figure 3b, d); this aligns to previous experimental findings <sup>30</sup>. Moreover, in the conduction state an inter-chain charge density can also be noticed.



**Figure 3.** Spatial distribution of charge of (a)(c) the highest valence state for monoclinic and orthorhombic structure, respectively and (b)(d) the lowest conduction state for monoclinic and orthorhombic structure, respectively

The observed spatial distribution of the conduction state is like that observed in the same kind of study on PE <sup>30</sup>, where it is reported a clear inter-chain character. In that study the delocalization of the charge has been related to the formation of localized

surface states inside the band gap, which allow electrons to be acquired and retained<sup>30</sup>. Based on this, additional studies on the surface electronic properties of PTFE will be conducted to explore its surface properties and their implications for interfacial interactions and the control of *e.g.* adhesion, wettability and triboelectrical response.

#### 4. CONCLUSIONS

In this study, we used a first-principles approach to give, for the first time, insights on the structural and electronic properties of PTFE in its high-pressure phase. We confirmed that, at high pressure the PTFE at form III (zigzag planar) coexists in orthorhombic and monoclinic crystal structures.

- I. The optimization of the lattice structures and the comparisons of the energy values obtained by adopting three different exchange-correlation functional (PZ, PBE and PBE-D), show that the PBE-D functional better describes the structural properties of PTFE in the two high-pressure configurations.
- II. The addition of a dispersion term to model the long-range van der Waals interactions to the PBE functional overcomes the inability of PZ to estimate the short-range interactions and the failure of PBE to estimate intermolecular interactions.
- III. The analysis of the electronic properties on the optimized structures reveals that an electronic charge transfers from carbons to fluorines inside the monomers. The charge is rearranged inside the stem and tends to concentrate around the fluorine atoms.
- IV. The band gap is estimated around 5 eV, which is comparable with some experimental findings but less with other previous theoretical and experimental studies because of the limits of the gradient-corrected (LDA/GGA) to calculate the insulating band gap. For both monoclinic and orthorhombic structure, the band gap is direct. Additional investigation of the band structures shows that the dispersion of both valence and conduction bands is not significantly affected by the functionals and cells structure adopted. The further DOS's calculations perfectly align with previous UPS and optical experimental analysis.
- V. By focusing on the PBE-D functional calculations it can be seen that charge distribution of the valence state is localized inside the PTFE stem and instead the conduction band is delocalized along the entire length of the chain and between the chains. The inter-chain character of the conduction state reported here is like the inter-chain character reported by similar study on PE. This suggests that, as for the PE, surface states might be generated on PTFE surface.

This study paves the way to clarify the properties of one of the most popular polymers available and to eventually exploit it for new advanced technologies.

## AUTHOR INFORMATION

### Corresponding author

\*E-mail: aciniero@unimore.it

### ORCID

Ciniero Alessandra: 0000-0002-2674-0491

### Notes

The authors declare no competing financial interest.

## ACKNOWLEDGMENTS

This research was supported by European Union Horizon 2020 Marie Curie Actions Grant Agreement No. 798245 for Dr. Ciniero, the UK Engineering and Physical Research Sciences Research Council (EPSRC – Doctoral Fellowship Prize for Dr. Ciniero and Prof. Dini's Established Career Fellowship EP/N025954/1) and the Taiho Kogyo Tribology Research Foundation (TTRF). Computational resources have been provided by the supercomputing facilities CINECA consortium and Imperial College London Research Computing Service (RCS). The authors would like to thank Prof Carlo Calandra for useful discussions.

## REFERENCES

1. Wang, Z. L., Triboelectric Nanogenerators as New Energy Technology for Self-Powered Systems and as Active Mechanical and Chemical Sensors. *ACS nano* **2013**, 7, 9533-9557.
2. Su, Y.; Chen, J.; Wu, Z.; Jiang, Y., Low Temperature Dependence of Triboelectric Effect for Energy Harvesting and Self-Powered Active Sensing. *Appl. Phys. Lett.* **2015**, 106, 013114(1-5).
3. Burgo, T. A.; Ducati, T. R.; Francisco, K. R.; Clinckspoor, K. J.; Galembeck, F.; Galembeck, S. E., Triboelectricity: Macroscopic Charge Patterns Formed by Self-Arraying Ions on Polymer Surfaces. *Langmuir* **2012**, 28, 7407-7416.
4. Ciniero, A. Triboemission Mechanisms. Ph.D. dissertation, Imperial College London, London, UK, 2017.
5. Burgo, T. A.; Erdemir, A., Bipolar Tribocharging Signal During Friction Force Fluctuations at Metal–Insulator Interfaces. *Angew. Chem.* **2014**, 126, 12297-12301.
6. Nakayama, K., Tribocharging and Friction in Insulators in Ambient Air. *Wear* **1996**, 194, 185-189.
7. Puhan, D.; Nevshupa, R.; Wong, J. S. S.; Reddyhoff, T., Transient Aspects of Plasma Luminescence Induced by Triboelectrification of Polymers. *Tribol. Int.* **2019**, 130, 366-377.
8. Ciniero, A.; Dini, D.; Reddyhoff, T., An Experimental and Theoretical Approach to Study the Link between Triboemission and Tribocharging. *Bull. Am. Phys. Soc.* **2018**.

9. Burgo, T. A.; Silva, C. A.; Balestrin, L. B.; Galembeck, F., Friction Coefficient Dependence on Electrostatic Tribocharging. *Sci. Rep.* **2013**, *3*, 2384(1-8).
10. Rezende, C.; Gouveia, R.; Da Silva, M.; Galembeck, F., Detection of Charge Distributions in Insulator Surfaces. *J. Phys.: Condens. Matter* **2009**, *21*, 263002(1-19).
11. Ciniero, A.; Le Rouzic, J.; Reddyhoff, T., The Use of Triboemission Imaging and Charge Measurements to Study Dlc Coating Failure. *Coatings* **2017**, *7*, 129(1-10).
12. Lacks, D. J.; Sankaran, R. M., Contact Electrification of Insulating Materials. *J. Phys. D: Appl. Phys.* **2011**, *44*, 453001(1-15).
13. Baytekin, H.; Patashinski, A.; Branicki, M.; Baytekin, B.; Soh, S.; Grzybowski, B. A., The Mosaic of Surface Charge in Contact Electrification. *Science* **2011**, *333*, 308-312.
14. Baytekin, H. T.; Baytekin, B.; Incorvati, J. T.; Grzybowski, B. A., Material Transfer and Polarity Reversal in Contact Charging. *Angew. Chem. Int. Ed.* **2012**, *51*, 4843-4847.
15. Frišić, T.; James, S. L.; Boldyreva, E. V.; Bolm, C.; Jones, W.; Mack, J.; Steed, J. W.; Suslick, K. S., Highlights from Faraday Discussion 170: Challenges and Opportunities of Modern Mechanochemistry, Montreal, Canada, 2014. *Chem. Commun.* **2015**, *51*, 6248-6256.
16. Mokha, A.; Constantinou, M.; Reinhorn, A., Teflon Bearings in Base Isolation I: Testing. *J. Struct. Eng.* **1990**, *116*, 438-454.
17. Lancaster, J., Accelerated Wear Testing of Ptfе Composite Bearing Materials. *Tribol. Int.* **1979**, *12*, 65-75.
18. Daraio, C.; Nesterenko, V. F.; Herbold, E. B.; Jin, S., Strongly Nonlinear Waves in a Chain of Teflon Beads. *Phys. Rev. E* **2005**, *72*, 016603(1-9).
19. Grainger, D. W.; Stewart, C. W., Fluorinated Coatings and Films: Motivation and Significance. In *Fluorinated Surfaces, Coatings, and Films*, American Chemical Society: 2001; Vol. 787, 1-14.
20. Clark, D.; Kilcast, D., Study of Core and Valence Energy Levels of Ptfе. *Nature-Phys Sci* **1971**, *233*, 77-79.
21. Pireaux, J.; Riga, J.; Caudano, R.; Verbist, J.; Andre, J.; Delhalle, J.; Delhalle, S., Electronic Structure of Fluoropolymers: Theory and Esca Measurements. *J. Electron. Spectrosc. Relat. Phenom.* **1974**, *5*, 531-550.
22. Delhalle, J., Influence of Chemical Substitution on Energy Band Structure of Polyfluoroethylenes. *Chem. Phys. Lett.* **1974**, *27*, 306-314.
23. Delhalle, J.; Delhalle, S.; André, J.; Pireaux, J.; Riga, J.; Caudano, R.; Verbist, J., Electronic Structure of Linear Fluoropolymers: Theory and Esca Measurements Revisited. *J. Electron. Spectrosc. Relat. Phenom.* **1977**, *12*, 293-303.
24. Seki, K.; Tanaka, H.; Ohta, T.; Aoki, Y.; Imamura, A.; Fujimoto, H.; Yamamoto, H.; Inokuchi, H., Electronic Structure of Poly (Tetrafluoroethylene) Studied by Ups, Vuv Absorption, and Band Calculations. *Phys. Scr.* **1990**, *41*, 167-171.
25. Nakafuku, C.; Takemura, T., Crystal Structure of High Pressure Phase of Polytetrafluoroethylene. *Jpn. J. Appl. Phys.* **1975**, *14*, 599-602.
26. Roberts, R.; Rowe, R.; York, P., The Relationship between Young's Modulus of Elasticity of Organic Solids and Their Molecular Structure. *Powder Technol.* **1991**, *65*, 139-146.
27. Jia, B.-B.; Liu, X.-J.; Cong, P.-H.; Li, T.-S., An Investigation on the Relationships between Cohesive Energy Density and Tribological Properties for Polymer-Polymer Sliding Combinations. *Wear* **2008**, *264*, 685-692.

28. Dake, S.; Rajopadhye, N.; Bhoraskar, S., Evaluation and Characterisation of Chemically Modified Polymers as Secondary Electron Emitters. *J. Phys. D: Appl. Phys.* **1987**, *20*, 1631-1636.
29. Falk, J.; Fleming, R., Study of the Electronic Band Structure of Polyacetylene and the Polyfluoroethylenes. *J. Phys. C: Solid State Phys.* **1975**, *8*, 627-646.
30. Serra, S.; Tosatti, E.; Iarlari, S.; Scandolo, S.; Santoro, G., Interchain Electron States in Polyethylene. *Phys. Rev. B* **2000**, *62*, 4389-4393.
31. Wang, C.; Duscher, G.; Paddison, S. J., Electron Energy Loss Spectroscopy of Polytetrafluoroethylene: Experiment and First Principles Calculations. *Microscopy* **2013**, *63*, 73-83.
32. Morokuma, K., Electronic Structures of Linear Polymers. II. Formulation and Cnd0/2 Calculation for Polyethylene and Poly (Tetrafluoroethylene). *J. Chem. Phys.* **1971**, *54*, 962-971.
33. McCubbin, W., An Assessment of Polymer Band Structure Calculations. *Chem. Phys. Lett.* **1971**, *8*, 507-512.
34. Kasowski, R. V.; Hsu, W. Y.; Caruthers, E. B., Electronic Properties of Polyacetylene, Polyethylene, and Polytetrafluoroethylene. *J. Chem. Phys.* **1980**, *72*, 4896-4900.
35. Otto, P.; Ladik, J.; Förner, W., The Energy Band Structure of Polyfluoroethylene: Influence of Chemical Substitution and Conformation. *Chem. Phys.* **1985**, *95*, 365-372.
36. D'Amore, M.; Talarico, G.; Barone, V., Periodic and High-Temperature Disordered Conformations of Polytetrafluoroethylene Chains: An Ab Initio Modeling. *JACS* **2006**, *128*, 1099-1108.
37. D'Amore, M.; Auriemma, F.; De Rosa, C.; Barone, V., Disordered Chain Conformations of Poly (Tetrafluoroethylene) in the High-Temperature Crystalline Form I. *Macromolecules* **2004**, *37*, 9473-9480.
38. Lorenzen, M.; Hanfland, M.; Mermet, A., Poly (Tetrafluoroethylene) under Pressure: X-Diffraction Studies. *Nucl. Instrum. Methods Phys. Res., Sect. B* **2003**, *200*, 416-420.
39. Springborg, M.; Lev, M., Electronic Structures of Polyethylene and Polytetrafluoroethylene. *Phys. Rev. B* **1989**, *40*, 3333-3339.
40. Bunn, C.; Howells, E., Structures of Molecules and Crystals of Fluoro-Carbons. *Nature* **1954**, *174*, 549-551.
41. Weeks, J.; Clark, E.; Eby, R., Crystal Structure of the Low Temperature Phase (II) of Polytetrafluoroethylene. *Polymer* **1981**, *22*, 1480-1486.
42. Farmer, B.; Eby, R., Energy Calculations of the Crystal Structure of the Low Temperature Phase (II) of Polytetrafluoroethylene. *Polymer* **1981**, *22*, 1487-1495.
43. Sperati, C. A.; Starkweather, H. W., Fluorine-Containing Polymers. II. Polytetrafluoroethylene. In *Fortschritte Der Hochpolymeren-Forschung*, Springer: 1961, 465-495.
44. Brown, R., Vibrational Spectra of Polytetrafluoroethylene: Effects of Temperature and Pressure. *J. Chem. Phys.* **1964**, *40*, 2900-2908.
45. Flack, H., High-Pressure Phase of Polytetrafluoroethylene. *J Polymer Sci 2 Polymer Phys* **1972**, *10*, 1799-1809.
46. Eby, R.; Clark, E.; Farmer, B.; Piermarini, G.; Block, S., Crystal Structure of Poly (Tetrafluoroethylene) Homo-and Copolymers in the High Pressure Phase. *Polymer* **1990**, *31*, 2227-2237.
47. Perdew, J. P.; Zunger, A., Self-Interaction Correction to Density-Functional Approximations for Many-Electron Systems. *Phys. Rev. B* **1981**, *23*, 5048-5079.

48. Ernzerhof, M.; Scuseria, G. E., Assessment of the Perdew–Burke–Ernzerhof Exchange–Correlation Functional. *J. Chem. Phys.* **1999**, *110*, 5029-5036.
49. Grimme, S., Semiempirical Gga-Type Density Functional Constructed with a Long-Range Dispersion Correction. *J. Comput. Chem.* **2006**, *27*, 1787-1799.
50. Righi, M. C.; Scandolo, S.; Serra, S.; Iarlori, S.; Tosatti, E.; Santoro, G., Surface States and Negative Electron Affinity in Polyethylene. *Phys. Rev. Lett.* **2001**, *87*, 076802(1-4).
51. Monkhorst, H. J.; Pack, J. D., Special Points for Brillouin-Zone Integrations. *Phys. Rev. B* **1976**, *13*, 5188-5192.
52. Tang, W.; Sanville, E.; Henkelman, G., A Grid-Based Bader Analysis Algorithm without Lattice Bias. *J. Phys.: Condens. Matter* **2009**, *21*, 084204(1-7).
53. Sanville, E.; Kenny, S. D.; Smith, R.; Henkelman, G., Improved Grid-Based Algorithm for Bader Charge Allocation. *J. Comput. Chem.* **2007**, *28*, 899-908.
54. Henkelman, G.; Arnaldsson, A.; Jónsson, H., A Fast and Robust Algorithm for Bader Decomposition of Charge Density. *Comput. Mater. Sci* **2006**, *36*, 354-360.
55. Yu, M.; Trinkle, D. R., Accurate and Efficient Algorithm for Bader Charge Integration. *J. Chem. Phys.* **2011**, *134*, 064111(1-8).
56. Brown, E.; Trujillo, C.; Gray III, G.; Rae, P.; Bourne, N., Soft Recovery of Polytetrafluoroethylene Shocked through the Crystalline Phase I-II Transition. *J. Appl. Phys.* **2007**, *101*, 024916.
57. Murnaghan, F., The Compressibility of Media under Extreme Pressures. *PNAS* **1944**, *30*, 244-247.
58. Perdew, J. P.; Levy, M., Physical Content of the Exact Kohn-Sham Orbital Energies: Band Gaps and Derivative Discontinuities. *Phys. Rev. Lett.* **1983**, *51*, 1884-1887.

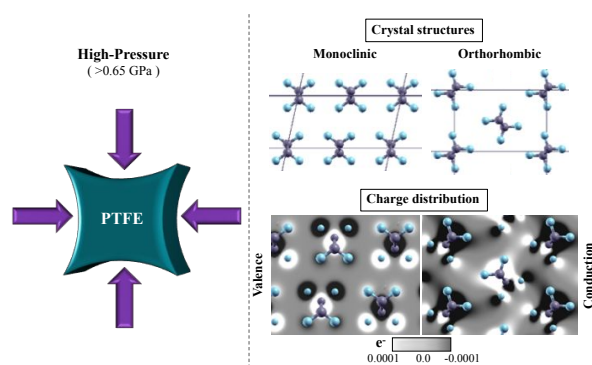


Table of Contents Graphic